

η^1 -Allylpalladium complexes with a tridentate PNP ligand with different phosphino groups†Bruno Crociani,^{*a} Simonetta Antonaroli,^a Paola Paoli^b and Patrizia Rossi^b

Received 4th April 2012, Accepted 15th August 2012

DOI: 10.1039/c2dt30746d

The iminodiphosphine 2-(PPh₂)C₆H₄-1-CH=NC₆H₄-2-(PPh₂) (P–N–P') is used for the preparation of the complexes [Pd(η^1 -CHR¹-CH=CHR²R³)(P–N–P')]BF₄ [R¹ = R² = R³ = H: (1); R¹ = R² = Ph, R³ = H: (2); R¹ = R³ = H, R² = Ph: (3); R¹ = H, R² = R³ = Me: (4)]. The P–N–P' tridentate coordination and the η^1 -allyl bonding mode in the solid are confirmed by the X-ray structural analysis of **1**. In solution, the complexes **1** and **2** undergo an η^1 - η^3 - η^1 rearrangement at 298 K interconverting the bonding site of the allyl group. A five-coordinate structure with the phosphine ligands in the axial position is proposed for the η^3 -allyl intermediate. For the dynamic process, a ΔG^\ddagger value of 53.8 kJ mol⁻¹ is obtained from ¹H NMR data of **2**. In **3** and **4**, the allyl ligand is rigidly bound to the metal through the less substituted terminus, in line with the higher free energy content of the corresponding isomers: [Pd(η^1 -CHPh-CH=CH₂)(P–N–P')] + 48.78 kJ mol⁻¹; [Pd(η^1 -CMe₂-CH=CH₂)(P–N–P')] + 69.35 kJ mol⁻¹. The complexes react with secondary amines in the presence of fumaronitrile at different rates yielding allylamines and the palladium(0) derivative [Pd(η^2 -fn)(P–N–P')] (**5**). On the basis of charge distribution on the allylic carbon atoms and of steric factors, the difference in rate and the regioselectivity in the amination of **1–3** are better rationalized by a mechanism with nucleophilic attack at the η^3 -intermediate rather than by an S_N2 mechanism with nucleophilic attack at the Pd–CHR¹ carbon atom. The high regioselectivity in the reaction of **4** with piperidine implies an S_N2' mechanism with nucleophilic attack at the CMe₂ allyl carbon. A dynamic process occurs also for the 18-electron complex **5** consisting in a dissociation–association equilibrium of the olefin.

Introduction

The η^1 -allylpalladium complexes so far reported in the literature have been identified in solution¹ by ¹H and ¹³C NMR spectroscopy, and some of them have also been isolated and characterized in the solid state mainly by X-ray diffraction analysis.^{1a,b,i,2} The configuration of the solid compounds depends on the nature of the other ligands in the molecule. With neutral monodentate or bidentate ligands the complexes are of the type [Pd(η^1 -allyl)-(η^3 -allyl)L],^{1h} *trans*-[PdCl(η^1 -allyl)L₂]^{1a,i} or [PdX(η^1 -allyl)-(L–L')]^{1b,c,2c-g,j} (X = aryl group or chloride ion), while with anionic or neutral tridentate ligands the complexes are of the type [Pd(η^1 -allyl)(L–Y–L')]^{1j} and [Pd(η^1 -allyl)(L–L'–Y)]²ⁱ (Y being the atom formally bearing a negative charge) or [Pd(η^1 -allyl)(L–L'–L'')]^{1e-g,2a,b,h}. In most cases, the complexes are fluxional in solution as they undergo a dynamic η^1 - η^3 - η^1 process, the η^3 -allylic species being formed by displacement of a

monodentate ligand or of a tooth of the bidentate and tridentate ligands. The η^1 -allyl group was found to react with secondary amines at lower rates with respect to the η^3 -bound ligand.^{1i,2i,3} From the regioselectivity of the nucleophilic attack it was inferred that both the S_N2 and S_N2' mechanisms are operative. On the basis of theoretical calculation, however, it has been reported that the η^1 -allyl ligand is unreactive toward nucleophiles.⁴ Actually, the η^1 -allyl ligand is susceptible to electrophilic attack by maleic anhydride^{1c} or by aldehydes and imines, the latter reactions being involved in catalytic processes.^{1j,4a,5} Due to our interest in the chemistry and catalytic properties of palladium derivatives with iminophosphine ligands,⁶ we have recently published a synthetic and structural work on the η^1 -allyl complexes [Pd(η^1 -CHR¹-CH=CHR²)(P–N–O)] (R¹ = R² = H, Ph; R¹ = H, R² = Ph; P–N–O as the anion derived from deprotonation of the hydroxylic group of 2-(PPh₂)C₆H₄-1-CH=NC₆H₄-2-OH).²ⁱ As a continuation of our studies, we wish to report herein the preparation and structural characterization in solution and in the solid state of the complexes [Pd(η^1 -allyl)(P–N–P')]BF₄ and [Pd(η^2 -fumaronitrile)(P–N–P')] (allyl = C₃H₅, 1,3-Ph₂C₃H₃, 3-PhC₃H₄, 3,3-Me₂C₃H₃; P–N–P' as the iminodiphosphine ligand 2-(PPh₂)C₆H₄-1-CH=NC₆H₄-2-(PPh₂)), where the diphenylphosphino groups have different substituents. The reactions of the η^1 -allyl complexes with diethylamine and piperidine have also been studied in order to get a better understanding of

^aDipartimento di Scienze e Tecnologie Chimiche, Università di Roma "Tor Vergata", Via delle Ricerca Scientifica, 00133 Roma, Italy.

E-mail: crociani@stc.uniroma2.it; Fax: +39 06 72594328

^bDipartimento di Energetica, Università di Firenze, Via S. Marta 3, 50139 Firenze, Italy

† Electronic supplementary information (ESI) available. CCDC 866113. For ESI and crystallographic data in CIF or other electronic format see DOI: 10.1039/c2dt30746d

the factors governing the mechanism and regioselectivity of amination.

Results and discussion

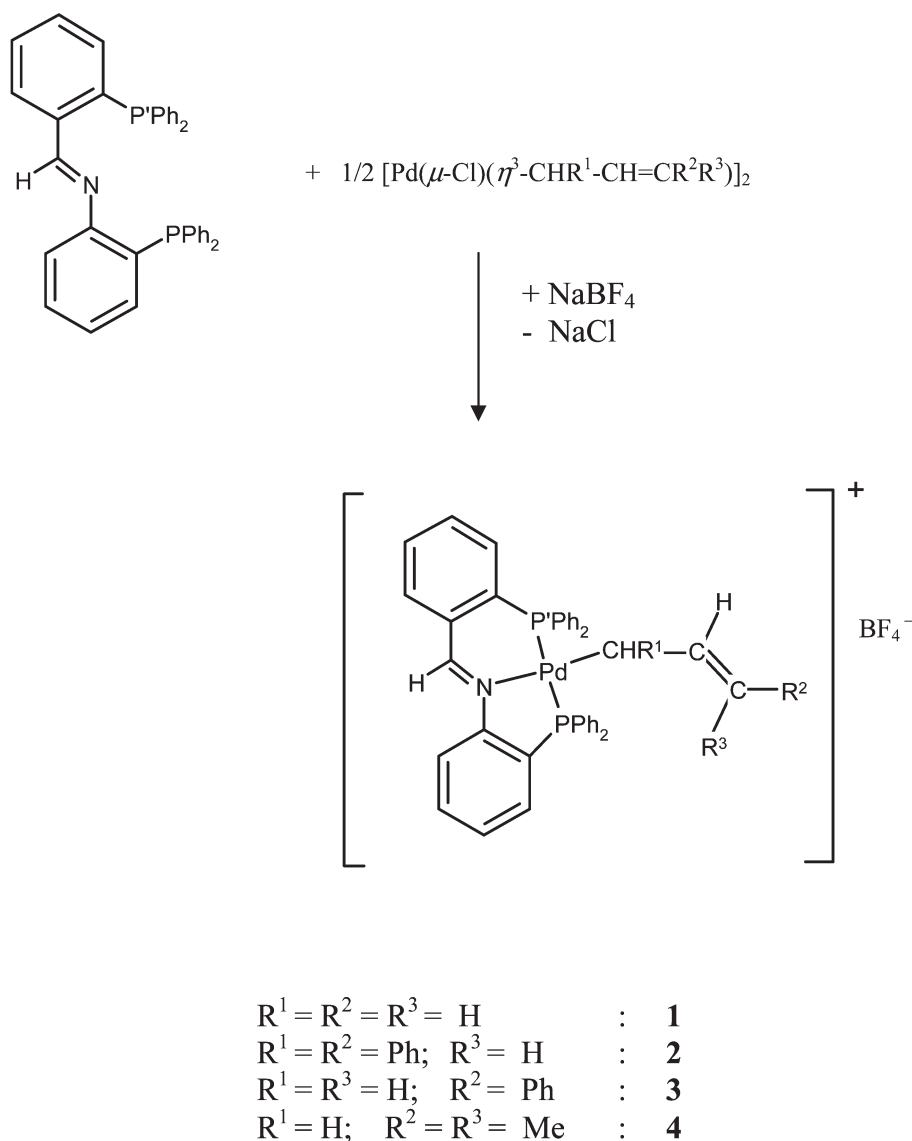
Preparation and solution behavior of the η^1 -allyl complexes

The η^1 -allylpalladium complexes **1–4** can be prepared from the reaction of the iminodiphosphine ligand P–N–P' with the η^3 -allyl dimers $[\text{Pd}(\mu\text{-Cl})(\eta^3\text{-CHR}^1\text{-CH=CR}^2\text{R}^3)]_2$ ($\text{R}^1 = \text{R}^2 = \text{R}^3 = \text{H}$; $\text{R}^1 = \text{R}^2 = \text{Ph}$, $\text{R}^3 = \text{H}$; $\text{R}^1 = \text{R}^3 = \text{H}$, $\text{R}^2 = \text{Ph}$; $\text{R}^1 = \text{H}$, $\text{R}^2 = \text{R}^3 = \text{Me}$) (molar ratio P–N–P'/Pd = 1 : 1) in the presence of sodium tetrafluoroborate as reported in Scheme 1.

The complexes **1–4** have been isolated in high yields and characterized by conductivity measurements, elemental analysis, IR, ^1H and ^{31}P NMR spectroscopy (see the Experimental section). The tridentate coordination of the ligand through the imino nitrogen and the phosphorus atoms is clearly indicated by

the low-frequency shift of the $\nu(\text{C}=\text{N})$ band ($17\text{--}20\text{ cm}^{-1}$) relative to the free ligand [$\nu(\text{C}=\text{N}) = 1621\text{ cm}^{-1}$] in the IR spectra, and by the appearance of the ^{31}P signals as AB quartets in the range 26–34 ppm with $^2J(\text{P-P})$ values of 312–362 Hz, which are typical of the non-equivalent ^{31}P nuclei in the *trans* position (Table 1).⁷ The PNP coordination is also confirmed by the X-ray structural analysis of complex **1** (see further).

Complexes **1** and **2** are fluxional in solution as they undergo a rapid (on the NMR time scale) $\eta^1\text{-}\eta^3\text{-}\eta^1$ exchange process which interconverts the four terminal allyl protons of **1** and the two terminal allyl protons of **2**. As can be seen in the ^1H NMR spectra of **1** in CD_2Cl_2 in the range 2–6 ppm (Fig. 1) at 298 K, the terminal allyl protons appear as a broad band centered at 3.30 ppm and the central proton as a quintet at 5.45 ppm. At 213 K, the exchange rate is considerably reduced and four signals are observed for the η^1 -allyl group at chemical shifts that one would expect by comparison with η^1 -allyl palladium complexes reported in the literature.^{1,2} In particular, the Pd–CH₂



Scheme 1

Table 1 Proton resonances of the allyl ligand in complexes 1–4,^a and ³¹P NMR data

Complex	T/K	Pd–CHR ¹	=CR ² R ³	=CH	³¹ P ^b
1 (R ¹ = R ² = R ³ = H)	298		3.30(br)	5.45	27.1d, 32.2d(br) (332) ^c 26.2d, 34.2d (362) ^c
	243				
2 (R ¹ = R ² = Ph; R ³ = H)	213	2.34ddd (5.5) ^f , (6.7) ^f , (6.7) ^g	3.74d ^d (16.7) ^g , 4.22d ^e (9.9) ^g	5.29m	22.0d(br), 26.0d(br) (312) ^c
	298		5.40(br)	mk ^h	
3 (R ¹ = R ³ = H; R ² = Ph)	213	4.45ddd (5.2) ^f , (14.0) ^f , (14.0) ^g	5.91d (14.0) ^g	mk ^h	23.1d, 31.5d (350) ^c
	298	2.70ddd (6.0) ^f , (6.0) ^f , (8.4) ^g	5.23d (15.6) ^g	5.84 dt (15.6) ^g , (8.4) ^g	
4 (R ¹ = H; R ² = R ³ = Me)	298	2.49ddd (5.9) ^f , (5.9) ^f , (8.5) ^g	0.83s, 1.19s	4.85t (8.5) ^g	24.8d, 28.5d (349) ^c

^a In CD₂Cl₂, chemical shifts in ppm and coupling constants in Hz. ^b AB system. ^c ³J(P–P). ^d Signal of proton *anti* to the central allylic proton. ^e Signal of proton *syn* to the central allyl proton. ^f ³J(P–H). ^g ³J(H–H). ^h Masked by the allyl proton resonance.

resonance appears as a rather broad multiplet due to coupling with the two non-equivalent phosphorus atoms and with the central allyl proton. Actually, this band consists of two overlapping triplets resulting from one of the ³J(P–H) coupling constants being equal to ³J(H–H) (Table 1).

The dynamic behavior of complex 1 was further examined by ³¹P NMR spectra at different temperatures (Fig. 2).

At 243 K, when the η¹-allyl form predominates, a rather sharp AB quartet is observed. On raising the temperature in the range 260–300 K, the two singlets at lower field progressively broaden and then become again sharper at 308 K, and even more at higher temperatures, while the two singlets at higher field remain almost unchanged. This trend can be rationalized in terms of a temperature-dependent equilibrium between the η¹-allyl complex and an η³-allyl intermediate, the latter being characterized by a ³¹P AB quartet with the two high-field singlets almost coincident with those of the η¹-allyl species and the two low-field singlets rather close to those of the η¹-allyl species. It is interesting to note that under conditions of fast exchange (at temperatures higher than 338 K) a ²J(P–P) coupling constant of 338 Hz is still detected which indicates that no Pd–P bond breaking occurs in

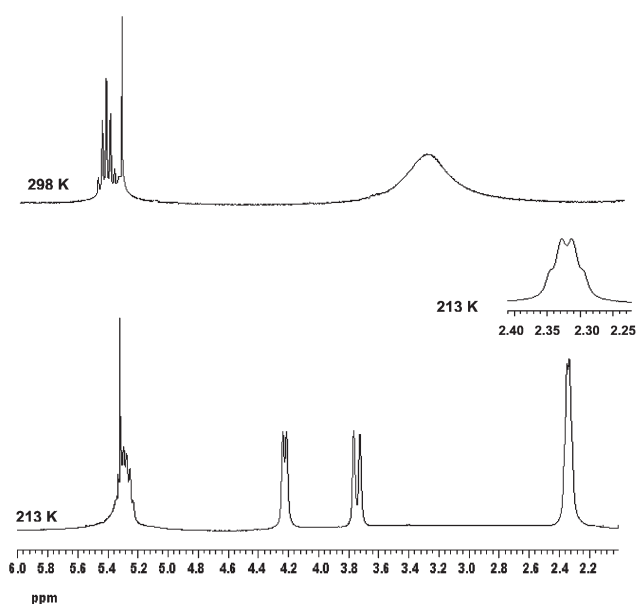


Fig. 1 ¹H NMR spectra (allyl region) of [Pd(η¹-C₃H₅)(P–N–P')]BF₄ (1) in CD₂Cl₂ at different temperatures.

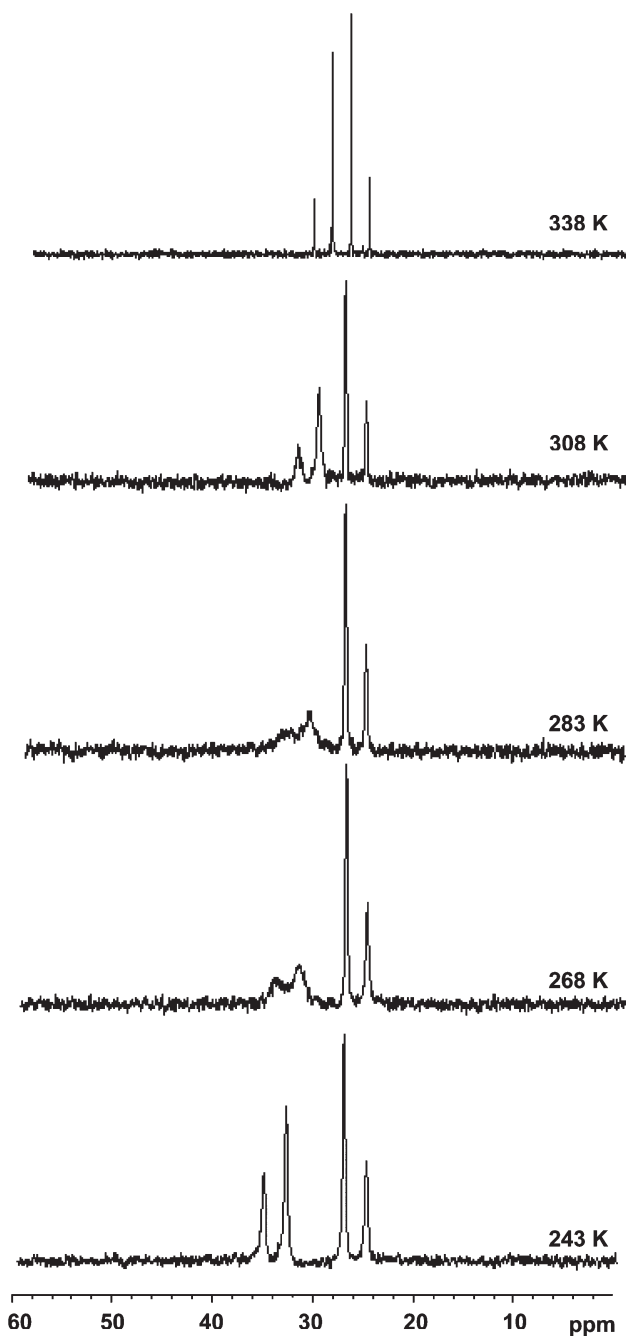


Fig. 2 ³¹P NMR spectra of [Pd(η¹-C₃H₅)(P–N–P')]BF₄ (1) at different temperatures (range 243–308 K: solvent CD₂Cl₂; 338 K: solvent DMSO-d₆).

the dynamic process and that a *trans* P–Pd–P structure is present in the η^3 -allyl intermediate.

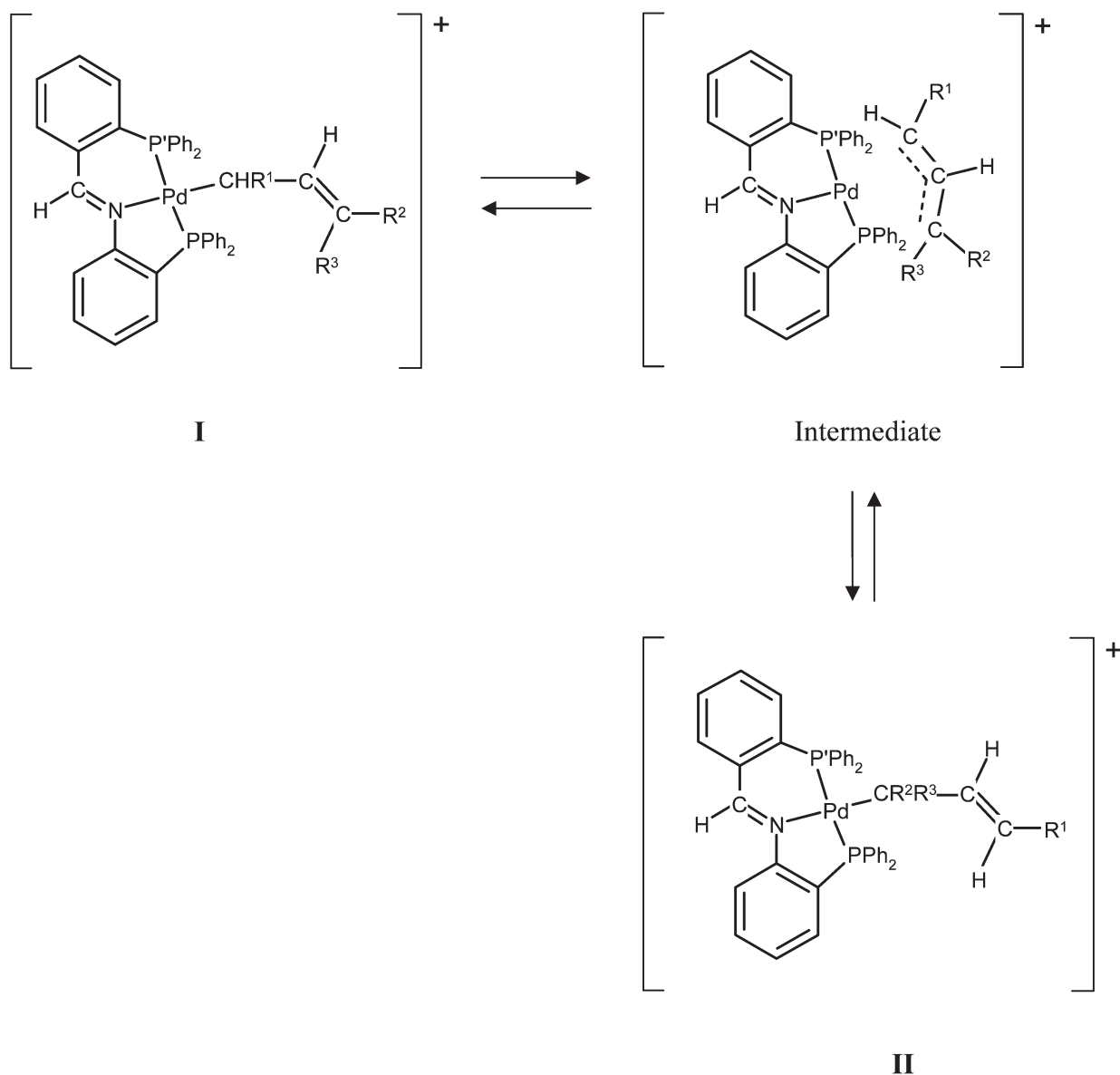
The occurrence of AB spin systems (due to the two non-equivalent phosphorus atoms linked to the same metal center) is confirmed by a 2D COSY experiment on the ^{31}P NMR spectrum of **1** in DMSO- d_6 at 318 K which shows correlation peaks between the signals of the AB quartet, namely between the two higher field signals at 22.72 and 25.53 ppm, between the two lower field signals at 29.03 and 31.84 ppm, between the signal at 22.72 ppm and that at 31.84 ppm, and between the signal at 25.53 ppm and that at 29.03 ppm.

In the ^1H NMR spectrum of **2** in CD_2Cl_2 at 213 K (Table 1), the terminal allyl proton CHPh resonates as a doublet at 5.91 ppm (with a $^3J(\text{H}-\text{H})$ of 14.0 Hz typical of a *trans*-CH=CH fragment), while the Pd–CHPh proton resonates as a multiplet at 4.45 ppm resulting from the overlap of three doublets (with $^3J(\text{H}-\text{H}) = ^3J(\text{P}-\text{H}) = 14.0$ Hz and $^3J(\text{P}-\text{H}) = 5.2$ Hz).

On raising the temperature to 290 K, the two signals coalesce into a single absorption at 5.4 ppm. From these data, a ΔG^\ddagger value of 53.8 kJ mol $^{-1}$ can be estimated for the dynamic process.⁸

On the basis of the above ^1H NMR data we propose the mechanism reported in Scheme 2 for the η^1 – η^3 – η^1 exchange process which interconverts the bonding site of the allyl ligand. The η^3 -intermediate is formulated as a five-coordinate species with the phosphine ligands in the axial position and with the imino nitrogen and the terminal allyl carbons on the equatorial plane. Such an intermediate, however, is never observed even when the temperature is lowered suggesting an equilibrium shift toward the η^1 bonding mode at low temperatures, which is the bonding mode found in the solid for complex **1** according to the X-ray structural data.

In contrast to the dynamic behavior of **1** and **2**, complexes **3** and **4** exhibit sharp ^1H and ^{31}P NMR spectra at 298 K, which



Scheme 2

are typical of “frozen” η^1 -allyl species with the allyl group bound to the central metal through the unsubstituted terminal carbon atom.^{2b,d,i} In both cases, the Pd–CH₂ proton resonance shows a $^3J(\text{H–H})$ coupling with the central allyl proton and two equal $^3J(\text{P–H})$ couplings with the *cis* phosphorus atoms (Table 1). In addition, the $^3J(\text{H–H})$ value of 15.6 Hz between the central and the terminal allyl protons is indicative of their *trans* position in the CH=CHPh unit of **3**. In order to check the occurrence of equilibria of Scheme 2 also for these complexes with asymmetrically substituted allyl ligands, we have recorded the ¹H NMR spectra of **4** in DMSO-*d*₆ in the temperature range 298–390 K. On increasing the temperature above 350 K, the two sharp singlets at 1.10 and 0.80 ppm for the methyl protons of the allyl ligand progressively broaden. Even though the coalescence was not complete due to decomposition at higher temperature, the change in shape of the signals suggests a slow exchange of the methyl groups which can take place in the isomeric structure **II** of Scheme 2, when the allyl ligand is η^1 -bound to the metal through the more substituted carbon atom. An analogous interconversion of the methyl groups through η^1 – η^3 – η^1 rearrangement was earlier reported for the complex [Pd(η^1 -CH₂-CH=CMe₂)(PNP)]BF₄ (PNP = 1,2-bis[(di-phenylphosphino)-methyl]pyridine).^{2b} On the basis of the above data, however, the equilibria of Scheme 2 for **4** (and presumably for **3**) involve undetectable amounts of the η^3 -intermediate and of the isomer **II**.

With the results from the solution studies on complexes **3** and **4** in mind, we set up a DFT modelling study aiming to evaluate the relative energy contents of the corresponding unsymmetrical isomers **I** and **II** which are involved in the equilibria of Scheme 2.

First of all, the suitability of the model chemistry adopted (see the Experimental section) was checked by comparing the experimental X-ray structure of [Pd(η^1 -C₃H₅)(P–N–P')]⁺ (**1**) (see later) with the optimized one **II**. The overall shape of the latter is consistent with the corresponding experimental one, thus confirming the reliability of the model chemistry. In particular, the experimental 3D arrangement of the η^1 -bound allyl ligand and the palladium coordination sphere is properly reproduced in the corresponding optimized structure (**1** vs. **II** in Table 2) as well as the relative orientation of the PPh₂ aromatic rings.

Importantly, although the Pd–donor atom bond distances are invariably slightly longer in comparison with the experimental values (Table 2), the allyl anion is doubtlessly η^1 -coordinated. In addition, the angle between the allyl plane and the mean plane described by the palladium centre with its four donor atoms well compares with the experimental one (66.4 vs. 66.1(7)°).

As for the complexes **3** and **4**, both isomers **I** (Fig. 3), corresponding to a Pd–CH₂ η^1 -coordination mode, are significantly more stable with respect to isomers **II**, the latter being +48.78 and +69.35 kJ mol^{–1} higher in energy, respectively, in agreement with the “frozen” η^1 -allyl species observed in the NMR spectra. This regioselectivity could be ascribed to obvious steric reasons (CH₂ vs. CHPh and CMe₂) and also to electronic factors, the terminal CH₂ carbon atom being more negatively charged with respect to the CHPh and CMe₂ allyl carbons in the corresponding unbound allyl anions (Table 3), as estimated by the Mulliken and Merz–Singh–Kollman charge derivation scheme (implemented in the Gaussian package).⁹

Table 2 Most significant geometrical parameters (Å, °) defining the coordination geometry of the palladium atom in complexes **II**, **3I** and **4I**, as derived from DFT calculations. For comparative purposes, experimental data derived from X-ray single crystal data of **1** are also reported (for atom labelling refer to Scheme 2)

Complex	II	[Pd(η^1 -C ₃ H ₅)(P–N–P')] ⁺ (1)	3I	4I
Pd–P	2.362	2.268(2)	2.364	2.365
Pd–N	2.233	2.156(7)	2.245	2.251
Pd–P'	2.363	2.304(2)	2.369	2.372
Pd–CHR ¹	2.098	2.065(8)	2.107	2.106
P–Pd–N	80.3	83.0(2)	80.2	80.3
P–Pd–P'	166.9	171.47(9)	166.3	166.4
N–Pd–P'	87.1	90.0(2)	86.4	86.6
P–Pd–CHR ¹	96.3	91.4(2)	96.4	96.9
P'–Pd–CHR ¹	96.3	95.7(2)	97.0	96.2
N–Pd–CHR ¹	176.6	173.9(3)	176.5	176.7

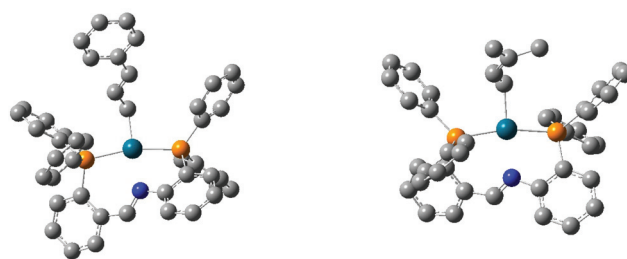


Fig. 3 Ball and stick representations of the DFT optimized complexes: **3I** [Pd(η^1 -CH₂-CH=CHPh)(P–N–P')]⁺ (left) and **4I** [Pd(η^1 -CH₂-CH=CMe₂)(P–N–P')]⁺ (right).

Within each couple of isomers (**3I** and **3II**, **4I** and **4II**), while the overall architecture of the complex is almost identical (data provided in the ESI†), in the **I** species the palladium–donor atom bond distances are always a little bit shorter than in the corresponding **II** ones. Finally, as expected, there are not significant differences in the palladium coordination sphere of the complexes **II**, **3I** and **4I** given that in all cases the metal is η^1 -bound to a CH₂ moiety (Table 2).

Solid state molecular structure of complex [Pd(η^1 -C₃H₅)(P–N–P')]BF₄·0.25Et₂O

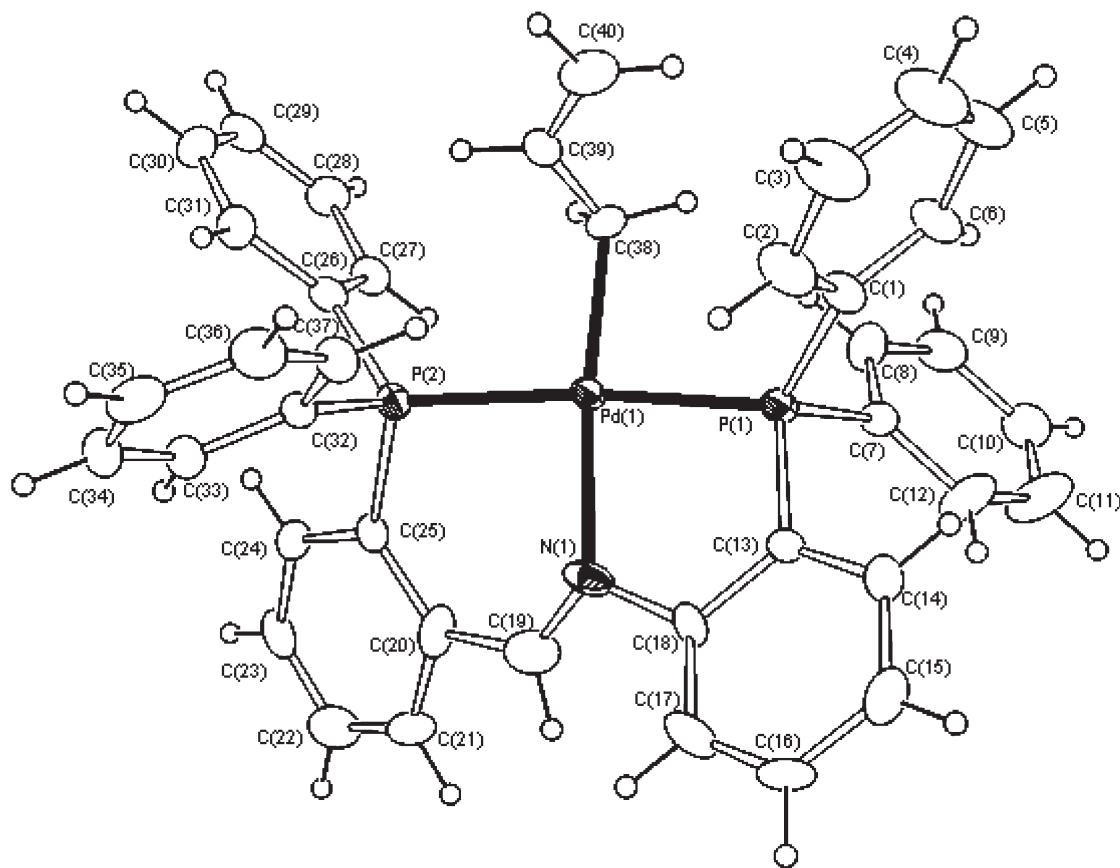
In the asymmetric unit of [Pd(η^1 -C₃H₅)(P–N–P')]BF₄·0.25Et₂O there is one complex cation **1**, one BF₄[–] counterion and a quarter of a diethyl ether molecule. The palladium ion in the [Pd(η^1 -C₃H₅)(P–N–P')]⁺ complex is four-coordinated by two *trans* disposed phosphorus atoms, by the nitrogen atom of the tridentate ligand and by the η^1 -allyl group (Fig. 4).

The coordination geometry is close to square-planar with the maximum deviation from the mean plane defined by the four donor atoms and the palladium atom of 0.123(8) Å (N(1)). Table 4 lists selected bond distances and angles in the [Pd(η^1 -C₃H₅)(P–N–P')]⁺ cation.

In order to compare the geometrical data observed in **1** with similar metal complexes, a literature survey was made. 13 complexes containing an η^1 -allylpalladium group were retrieved and of these just two^{2b,h} contain a PNP type ligand. More in general, only 4 metal complexes were found which feature a ligand

Table 3 Atomic charges (*e*) calculated by using the Mullikan (M) and Merz–Singh–Kollman (MSK) schemes (HF/6-31G* and B3LYP/6-31G* model chemistries)

	HF/6-31G*			B3LYP/6-31G*		
Isolated allyl anion	CR ² R ³ (M/MSK)	CH (M/MSK)	CHR ¹ (M/MSK)	CR ² R ³ (M/MSK)	CH (M/MSK)	CHR ¹ (M/MSK)
C ₃ H ₅ [−]	−0.623/−1.188	+0.030/+0.525	−0.623/−1.188	−0.505/−1.041	+0.037/+0.394	−0.505/−1.041
PhCHCHCHPh [−]	−0.362/−0.760	−0.094/+0.282	−0.362/−0.760	−0.276/−0.489	−0.090/+0.067	−0.276/−0.489
CHPhCHCH ₂ [−]	−0.405/−0.837	−0.045/+0.279	−0.541/−0.874	−0.307/−0.631	−0.027/+0.144	−0.447/−0.740
Me ₂ CCHCH ₂ [−]	−0.121/−0.296	−0.039/−0.012	−0.624/−0.994	+0.101/−0.255	−0.068/−0.042	−0.501/−0.858
[Pd(η ¹ -allyl(P–N–P'))] ⁺ (most stable isomer)				CR ² R ³ (M)	CH (M)	CHR ¹ (M)
C ₃ H ₅	—	—	—	−0.352	−0.016	−0.404
PhCHCHCHPh	—	—	—	−0.199	−0.053	−0.338
CHPhCHCH ₂	—	—	—	−0.187	−0.070	−0.406
Me ₂ CCHCH ₂	—	—	—	+0.185	−0.126	−0.400

**Fig. 4** ORTEP3 view of the cation [Pd(η¹-C₃H₅)(P–N–P')]⁺. The ellipsoid probability was set to 30%. The atom labelling scheme used in the discussion of the X-ray structure is analogous to that used in ref. 2i.

having the same atomic sequence of the P–N–P' ligand reported in the present work (*i.e.* P–C–C–N–C–C–P, – being any type of bond), and only one of them has palladium as the metal centre,^{10a} while all the four complexes contain the same P–N–P'-ligand used in this work.^{7,10}

Bond distances and angles around the metal ion in **1** well compare with those already reported,¹¹ including the Pd–C(38) distance. In particular, as found in related compounds, the M–P(1) distance (where M is the coordinated metal atom and P(1) belongs to the five-membered chelate ring) is usually

shorter than the M–P(2) one (where P(2) is part of the six-membered chelate ring); the P–M–N angle belonging to the six-membered ring is always larger than that of the five-membered one, and finally the N–M–X and P–M–P angles are slightly less than 180°. ^{10a} The plane containing the allyl ligand forms an angle of 66.1(7)° with respect to the mean plane formed by the four donor atoms and the palladium centre. As for the five- and six-membered chelate rings, the non-donor atoms in the six-membered ring lie on the opposite side with respect to the non-donor atoms of the five-membered ring. Finally, the

Table 4 Selected bond distances (Å) and angles (°) for the cation [Pd(η^1 -C₃H₅)(P–N–P)]⁺ as derived from the X-ray diffraction data

Pd(1)–N(1)	2.156(7)
Pd(1)–P(1)	2.268(2)
Pd(1)–P(2)	2.304(2)
Pd(1)–C(38)	2.065(8)
N(1)–Pd(1)–P(1)	83.0(2)
N(1)–Pd(1)–P(2)	90.0(2)
N(1)–Pd(1)–C(38)	173.9(3)
P(1)–Pd(1)–P(2)	171.47(9)
P(1)–Pd(1)–C(38)	91.4(2)
P(2)–Pd(1)–C(38)	95.7(2)

conformations adopted by the two rings can be described as envelope (E₅ in the series N(1), C(18), C(13), P(1), Pd(1)) and twist boat (TB_{2,5} in the series P(2), C(25), C(20), C(19), N(1), Pd(1)), for the five and six-membered rings, respectively.¹² The C(18)–N(1)–C(19)–C(20) fragment, which connects the two aromatic rings of the P–N–P' ligand, lies on a plane and forms angles of 25.2(7) and 15.7(6)° with the C(13)–C(18) and C(20)–C(25) aromatic mean planes, respectively, while the two aromatic rings form with each other an angle of 40.9(3)°. The diphenylphosphino C(1)–C(6) and C(7)–C(12) aromatic ring mean planes form an angle of 66.3(3)°, while the other couple of phenyl rings (C(26)–C(31)/C(32)–C(37)) forms an angle of 76.0(3)°. Finally, the C(1)–C(6) and C(26)–C(31) rings are facing each other (they form an angle of 11.6(3)°) and the distance between their geometrical centroid (calculated using only the carbon atoms) is 8.41 Å. A C...H π interaction exists between the allyl group and the aromatic ring of one diphenylphosphino moiety: the distance of H(40a) from the centroid of the C(1)–C(6) ring (Ct, in the following) is 2.946(3) Å, while the angle C(40)–H(40a)...Ct is 140.7(7)°. Finally, in the crystal packing, due to the presence of π - π interactions between two symmetry related C(20)–C(25) aromatic rings (the symmetry operation is $-x + 1, -y, -z + 1$), dimers of the palladium complex are formed, the distance between the centroids of the rings being 3.88(1) Å.¹³

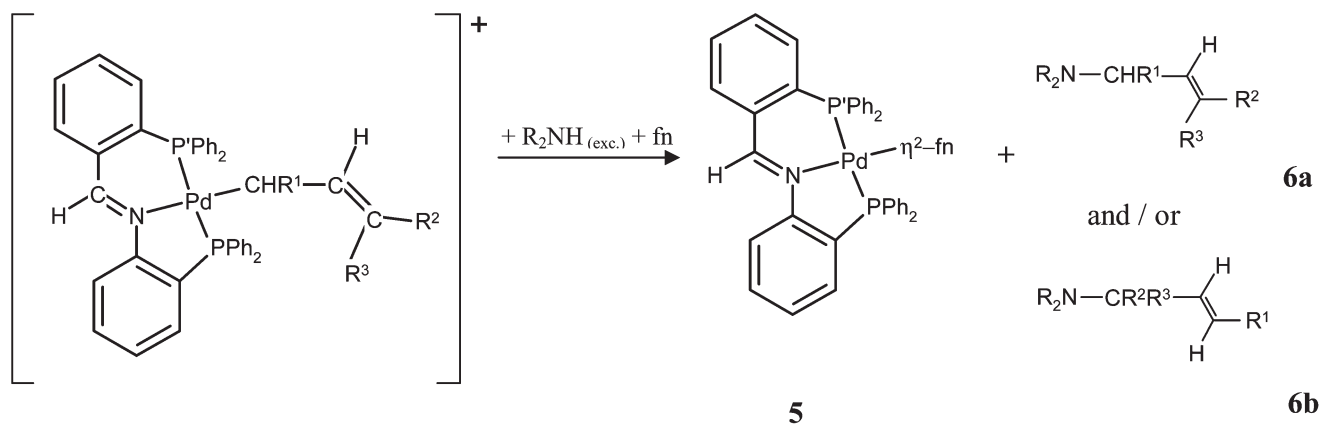
Allyl amination and characterization of [Pd(η^2 -fumaronitrile)-(P–N–P)]

The complexes **1–4** react with secondary amines (diethylamine or piperidine) in the presence of fumaronitrile (fn) yielding the palladium(0) derivative **5** and allylamines **6a** and/or **6b** (Scheme 3).

We have followed the course of the reaction and analyzed the products by means of ¹H and ³¹P NMR spectroscopy upon mixing the reactants in a molar ratio complex/R₂NH/fn of 1 : 5 : 1.2 at 298 K. The formation of **5** can be easily detected by its characteristic $\delta(^{31}\text{P})$ signals (see further), while the formation of **6a** and/or **6b** is indicated by the typical proton resonances of the allyl group. The results are summarized in Table 5.

From the completion times of the reactions with diethylamine it appears that complexes **1** and **2** react faster than **3** and **4**. A high selectivity occurs in the reactions of **3** with both amines (yielding the regioisomer **6a**) and of **4** with piperidine (yielding the regioisomer **6b**). According to literature reports, the observed regioselectivity would imply a nucleophilic attack at the Pd–CHR¹ carbon atom (S_N2 mechanism) for **3** and at the terminal =CR²R³ carbon atom (S_N2' mechanism) for **4**, respectively.^{1i,2j,3} In order to get a better understanding of the differences in rate and regioselectivity, we have calculated the charge distribution on the allyl carbon atoms of complexes **1–4** (Table 3).

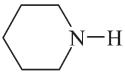
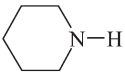
As one can see, in all cases the Pd–CHR¹ allyl carbon bears the highest negative charge which makes it more prone to an electrophilic attack rather than to a nucleophilic one. In fact, all the complexes undergo protonolysis of the Pd–CHR¹ bond by trace amounts of hydrochloric acid present in CDCl₃ yielding the cationic species [PdCl(P–N–P)]⁺.⁷ Thus, within the reliability of the data in Table 3, amination through an S_N2 mechanism can hardly take place by considering also the large steric requirements of the Pd(P–N–P) moiety. A partial negative charge is also present on the terminal allyl carbon =CR²R³ of complexes **1–3**, which renders unlikely a nucleophilic attack at this carbon atom through an S_N2' mechanism. A partial positive charge,



R₂NH = diethylamine or piperidine;
fn = fumaronitrile

Scheme 3

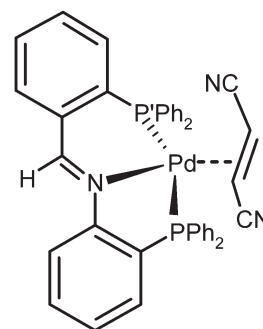
Table 5 Allyl amination data^a

Complex	R ₂ NH	Completion time	Allylamine ^b
1	Et ₂ NH	ca. 1 h	6a
2	Et ₂ NH	ca. 4 h ^c	6a
3	Et ₂ NH	ca. 9 h	6a
4	Et ₂ NH	Very slow	6a + 6b ^d
3		ca. 4 h	6a
4		ca. 12 h	6b

^a Experimental condition: complex/R₂NH/fn molar ratio of 1 : 5 : 1.2 in CDCl₃ at 298 K. ^b Predominant product (>98%) of allylation, within the limit of integration of the ¹H NMR signals. ^c In CD₂Cl₂. ^d Molar ratio 6a/6b of 9 : 1. This ratio remains almost constant during the course of the slow reaction, which is not complete even after 4 days.

however, is present on the terminal allyl carbon =CR²R³ (R² = R³ = Me) of **4**, which accounts for the regioselectivity observed in its reaction with piperidine (S_N2' mechanism). This finding parallels that reported by Åkermark for the reaction of dimethylamine with a mixture [PdCl(η³-CH₂-CH=CMe₂)₂]/PPh₃ (1 : 4 molar ratio).³ The higher reaction rates of the reactions of **1** and **2** with diethylamine (as compared to the corresponding reactions of **3**) and the regioselectivity in the reactions of **3** are better interpreted in terms of a nucleophilic attack occurring at the η³-allyl intermediate of Scheme 2, which is present in higher concentration in the solutions of **1** and **2** at 298 K according to ¹H NMR data. In literature data, the amination of cationic η³-allylpalladium complexes (allyl = CH₂-CH=CMe₂ or CH₂-CH=CHPh) was found to involve the less substituted allyl terminus.^{3,14} The steric requirements of the entering amine play an important role in the rates and regioselectivity to such an extent that the reaction of **4** with the more sterically hindered diethylamine is extremely slow and yields both regioisomers **6a** and **6b** in a molar ratio of 9 : 1. In this case, the rate of attack at the terminal=CMe₂ carbon of the η¹-allyl ligand (yielding **6b**) is considerably depressed by steric repulsion of the substituents, and becomes comparable (or even lower) to the rate of attack at trace amounts of the η³-allyl intermediate (yielding **6a**).

The complex **5** has been isolated in high yield and characterized by elemental analysis, IR, ¹H and ³¹P NMR spectroscopy (see the Experimental section). It appears to be an 18 electron palladium(0) derivative due to the tridentate coordination of the P-N-P' ligand and the η²-bonding mode of the olefin. As a matter of fact, the ³¹P resonances in CDCl₃ are detected as two doublets at 27.6 and 12.0 ppm, respectively, with a ²J(P-P) coupling of 18.7 Hz (which rules out a *trans*-P-Pd-P structure) while the imino proton signal is observed at 8.21 ppm (0.78 ppm upfield relative to the free ligand). Correspondingly, in the IR spectrum the ν(C=N) vibration at 1581 cm⁻¹ is markedly shifted to lower frequency as compared to the free ligand. The spectral change of the CH=N unit suggests extensive d → π* back donation upon N-coordination to the central metal. The presence of the coordinated olefin is further confirmed by the observation of a ν(C≡N) band at 2204 cm⁻¹ in the IR spectrum (*cf.* the corresponding vibration at 2244 cm⁻¹ of the free

**Fig. 5** Proposed structure for the complex [Pd(η²-fumaronitrile)-(P-N-P')] (**5**).

fumaronitrile). The ¹H NMR spectrum in CD₂Cl₂ at 298 K shows the presence of a broad singlet at 2.85 ppm for the protons of the η²-bound olefin and of a small singlet at 6.33 ppm for the protons of the free olefin with an integration ratio of 16 : 1. On cooling to 268 K, the proton signal of the coordinated olefin appears as two doublets of doublets of doublets centered at 2.94 ppm [³J(H-H) = ³J(P-H) = 9.0 Hz, ³J(P-H) = 3.7 Hz] and 2.83 ppm [³J(H-H) = ³J(P-H) = 8.9 Hz, ³J(P-H) = 2.9 Hz], respectively. The observed spectral change and the presence of non-equivalent olefin protons at low temperature may be accounted for by a dissociation-association equilibrium of the olefin which occupies a coordination site at a corner of a distorted tetrahedral structure as depicted in Fig. 5.

Conclusion

In the cationic complexes **1–4**, the iminodiphosphine 2-(PPh₂)-C₆H₄-1-CH=NC₆H₄-2-(PPh₂) (P-N-P') acts as a tridentate ligand as indicated by ¹H and ³¹P NMR data in solution, and by the X-ray structural analysis of **1** in the solid. The solution behavior of **1** and **2** (η¹-η³-η¹ process), as well as the amination data with secondary amines in the presence of fumaronitrile (difference in rate between **1** and **3**, and regioselectivity for complex **3**), are better rationalized on the basis of a penta-coordinate η³-intermediate with the phosphino groups in the axial position. In agreement with atomic charge calculation, the nucleophilic attack of piperidine occurs at the more substituted allyl carbon of the η¹-CH₂-CH=CMe₂ ligand of complex **4**. In addition to allylamines, the amination reactions yield the palladium(0) derivative **5** containing the tridentate P-N-P' ligand and the η²-bound fumaronitrile.

Experimental

¹H NMR spectra were recorded on Bruker AM400 or Bruker Avance 300 spectrometers operating at 400.13 and 300.13 MHz, respectively. ³¹P{¹H} NMR spectra were recorded on a Bruker Avance 300 spectrometer operating at 121.49 MHz. Chemical shifts are reported in ppm downfield from SiMe₄ for ¹H and from H₃PO₄ as an external standard for ³¹P. The spectra were run at 25 °C except when noted. IR spectra were recorded on a Perkin-Elmer Spectrum One FT-IR spectrometer. All the reactions were carried out under N₂. The solvents and the

commercially available chemicals, such as sodium tetrafluoroborate and fumaronitrile, were used without further purification. Diethylamine and piperidine were distilled over anhydrous K_2CO_3 under N_2 . The iminodiphosphine P–N–P' and the complexes $[Pd(\mu-Cl)(\eta^3-CHR^1-CH=CR^2R^3)]_2$ ($R^1 = R^2 = R^3 = H$; $R^1 = R^2 = Ph$, $R^3 = H$; $R^1 = R^3 = H$, $R^2 = Ph$; $R^1 = H$, $R^2 = R^3 = Me$) were prepared by literature methods.^{1a,15,16}

Preparation of $[Pd(\eta^1-CHR^1-CH=CR^2R^3)(P-N-P')]BF_4$ (1–4)

A solution of $NaBF_4$ (0.066 g, 0.6 mmol) in MeOH (5 cm³) was added to a solution of P–N–P' (0.275 g, 0.5 mmol) and $[Pd(\mu-Cl)(\eta^3-CHR^1-CH=CR^2R^3)]_2$ (0.25 mmol) in CH_2Cl_2 (20 cm³). The mixture was stirred for 2 h at room temperature and the solvent was evaporated to dryness at reduced pressure. The solid residue was extracted with CH_2Cl_2 (20 cm³). After addition of activated charcoal and filtration, the clear solution was concentrated to a small volume (ca. 3 cm³) and diluted with Et_2O to precipitate the solid products with colours ranging from yellow to purple. The complexes were purified by a further precipitation from $CH_2Cl_2-Et_2O$.

Complex 1 ($R^1 = R^2 = R^3 = H$): yellow solid (0.370 g, 94%) (found C 60.90, H 4.25, N 1.72; $C_{40}H_{34}BF_4NP_2Pd$ requires C 61.29, H 4.37, N 1.79%); A_M 51.1 S cm² mol⁻¹ for a 1×10^{-3} mol dm⁻³ solution in CH_2Cl_2 at 298 K; ν_{max} (Nujol)/cm⁻¹ 1603 (C=N), 1058 (B–F); δ_H (400 MHz, CD_2Cl_2 , 213 K) 2.34 (2 H, ddd, $^3J(H-H) = ^3J(P-H) = 6.7$ Hz, $^3J(P-H) = 5.5$ Hz, Pd–CH₂), 3.74 (1H, d, $^3J(H-H) = 16.7$ Hz, =CH₂ proton *trans* to the central allylic proton), 4.22 (1H, d, $^3J(H-H) = 9.9$ Hz, =CH₂ proton *cis* to the central allylic proton), 5.29 (1H, m, =CH, central allylic proton), 7.2–8.0 (28 H, m, aryl protons), 8.72 (1H, s, N=CH).

Complex 2 ($R^1 = R^2 = Ph$, $R^3 = H$): purple solid (0.412 g, 88%) (found C 66.42, H 4.40, N 1.45; $C_{52}H_{42}BF_4NP_2Pd$ requires C 66.72, H 4.52, N 1.50%); A_M 54.1 S cm² mol⁻¹ for a 1×10^{-3} mol dm⁻³ solution in CH_2Cl_2 at 298 K; ν_{max} (Nujol)/cm⁻¹ 1601 (C=N), 1058 (B–F); δ_H (400 MHz, CD_2Cl_2 , 213 K) 4.45 (1 H, ddd, $^3J(H-H) = ^3J(P-H) = 14.0$ Hz, $^3J(P-H) = 5.2$ Hz, Pd–CH₂), 5.91 (1H, d, $^3J(H-H) = 14.0$ Hz, =CHPh, proton *trans* to the central allylic proton), 6.4–8.0 (39 H, m, central allylic proton and aryl protons), 8.45 (1H, s, N=CH).

Complex 3 ($R^1 = R^3 = H$, $R^2 = Ph$): orange solid (0.414 g, 96%) (found C 64.21, H 4.28, N 1.57; $C_{46}H_{38}BF_4NP_2Pd$ requires C 64.24, H 4.45, N 1.63%); A_M 51.9 S cm² mol⁻¹ for a 1×10^{-3} mol dm⁻³ solution in CH_2Cl_2 at 298 K; ν_{max} (Nujol)/cm⁻¹ 1604 (C=N), 1064 (B–F); δ_H (300 MHz, CD_2Cl_2 , 298 K) 2.70 (2 H, ddd, $^3J(H-H) = 8.4$ Hz, $^3J(P-H) = 6.0$ Hz, Pd–CH₂), 5.23 (1 H, d, $^3J(H-H) = 15.6$ Hz, =CHPh, proton *trans* to the central allylic proton), 5.84 (1H, dt, =CH, central allylic proton), 6.7–6.9 (2 H, m, aryl protons), 7.0–7.3 (3 H, m, aryl protons), 7.4–8.3 (28 H, m, aryl protons), 8.86 (1H, s, N=CH).

Complex 4 ($R^1 = H$, $R^2 = R^3 = Me$): orange solid (0.340 g, 84%) (found: C 62.07, H 4.70, N 1.75; $C_{42}H_{38}BF_4NP_2Pd$ requires C 62.13, H 4.72, N 1.73%); $A_M = 55.2$ S cm² mol⁻¹ for a 1×10^{-3} mol dm⁻³ solution in CH_2Cl_2 at 298 K; ν_{max} (Nujol)/cm⁻¹ 1604 (C=N), 1058 (B–F); δ_H (300 MHz, CD_2Cl_2 , 298 K) 0.83 (3 H, s, CH₃), 1.19 (3 H, s, CH₃), 2.49 (2 H, ddd,

$^3J(H-H) = 8.5$ Hz, $^3J(P-H) = ^3J(P-H) 5.9$ Hz, Pd–CH₂), 4.85 (1 H, t, =CH, central allylic proton), 7.2–7.9 (27 H, m, aryl protons), 8.2–8.3 (1 H, m, aryl proton), 9.09 (1H, s, N=CH).

Preparation of $[Pd(\eta^2-fn)(P-N-P')]\cdot CH_2Cl_2$

Diethylamine (0.183 g, 2.5 mmol) was added to a solution of complex **1** (0.392 g, 0.5 mmol) and fumaronitrile (0.047 g, 0.6 mmol) in CH_2Cl_2 (20 cm³) under N_2 . After stirring for 2 h at room temperature, the mixture was treated with H_2O (2×10 cm³). The organic phase was dried over anhydrous Na_2SO_4 , concentrated to a small volume (ca. 5 cm³) and diluted with Et_2O to precipitate the product as a yellow-brown solid, which was purified by further precipitation from $CH_2Cl_2-Et_2O$. As shown by the ¹H NMR spectrum in acetone-d₆ and elemental analysis, the complex contains a CH_2Cl_2 molecule of crystallization (0.310 g, 76%) (found: C 61.33, H 4.05, N 5.07; $C_{42}H_{33}Cl_2N_3P_2Pd$ requires C 61.59, H 4.06, N 5.13%); ν_{max} (Nujol)/cm⁻¹ 2204 (C≡N), 1581 (C=N); δ_H (300 MHz, CD_2Cl_2 , 298 K) 2.85 (2 H, s, br, olefin protons), 6.7–6.8 (1 H, m, aryl proton), 6.9–7.0 (2 H, m, aryl protons), 7.0–7.1 (2 H, m, aryl protons), 7.1–7.6 (24 H, m, aryl protons), 7.7–7.8 (1 H, m, aryl proton), 8.20 (1 H, s, N=CH); δ_H (300 MHz, acetone-d₆, 298 K) 5.64 (2 H, s, CH_2Cl_2); δ_P (300 MHz, CD_2Cl_2 , 298 K) 11.7 d, 27.7 d, $^2J(P-P) = 16.7$ Hz.

Identification of allylamines **6a** and **6b**

The allylamines **6a** and **6b** formed in the reaction of complexes **1–4** with secondary amines (diethylamine or piperidine) in the presence of fumaronitrile were detected and characterized by the proton resonances of the allyl group in the ¹H NMR spectra and, in some cases, by GC-MS analysis of the reaction mixture.

Et₂N–CH₂–CH=CH₂ (3-diethylaminopropene) δ_H (300 MHz, $CDCl_3$, 298 K): 3.12 (2 H, d, $^3J(H-H) = 6.5$ Hz, N–CH₂), 5.14 (1 H, d, $^3J(H-H) = 10.9$ Hz, =CH₂ proton *cis* to the central allylic proton), 5.19 (1H, d, $^3J(H-H) = 18.1$ Hz, =CH₂ proton *trans* to the central allylic proton), 5.89 (1H, m, =CH, central allylic proton); MS data: m/z 113 (M^+ , 9%), 98 (68, M – CH₃), 86 (22, M – CH=CH₂), 84 (5, M – C₂H₅), 72 (3, M – CH₂CH=CH₂).

Et₂N–CHPh–CH=CHPh (*trans*-3-diethylamino-1,3-diphenylpropene) δ_H (300 MHz, $CDCl_3$, 298 K): 4.31 (1H, d, $^3J(H-H) = 8.8$ Hz, N–CHPh), 6.37 (1 H, dd, $^3J(H-H) = 8.8$, $^3J(H-H) = 15.8$, =CH, central allylic proton), 6.56 (1 H, d, $^3J(H-H) = 15.8$, =CHPh, proton *trans* to the central allylic proton).

Et₂N–CH₂–CH=CHPh (*trans*-3-diethylamino-1-phenylpropene) δ_H (300 MHz, $CDCl_3$, 298 K): 3.28 (2 H, d, $^3J(H-H) = 6.7$ Hz, N–CH₂), 6.32 (1 H, dt, $^3J(H-H) = 6.7$ Hz, $^3J(H-H) = 15.9$ Hz, =CH, central allylic proton), 6.53 (1 H, d, $^3J(H-H) = 15.9$ Hz, =CHPh, proton *trans* to the central allylic proton); MS data: m/z 189 (M^+ , 8%), 174 (6, M – CH₃), 160 (4, M – C₂H₅), 117 (66, M – N(C₂H₅)₂), 72 (2, M – CH₂CH=CHC₆H₅).

Et₂N–CH₂–CH=CMe₂ (4-diethylamino-2-methyl-2-butene) δ_H (300 MHz, $CDCl_3$, 298 K): 1.68 (s, CH₃), 1.76 (s, CH₃), 2.86 (d, $^3J(H-H) = 7.9$ Hz, N–CH₂), 5.28 (t, $^3J(H-H) = 7.9$ Hz, =CH, central allylic proton); MS data: m/z 141

(M⁺, 14%), 126 (25, M – CH₃), 86 (28, M – CH=C(CH₃)₂), 72 (17, M – CH₂CH=C(CH₃)₂).

Et₂N–CMe₂–CH=CH₂ (3-diethylamino-3-methyl-1-butene) δ_{H} (300 MHz, CDCl₃, 298 K): 1.16 (s, CH₃), 4.9–5.1 (m, =CH₂), 5.91 (dd, ³J(H–H) = 17.6 Hz, ³J(H–H) = 10.8 Hz, =CH, central allylic proton).

C₅H₁₀N–CH₂–CH=CHPh (*trans*-1-phenyl-3-piperidino-propene) δ_{H} (300 MHz, CDCl₃, 298 K): 3.14 (2 H, d, ³J(H–H) = 6.7 Hz, N–CH₂), 6.32 (1 H, dt, ³J(H–H) = 6.7 Hz, ³J(H–H) = 15.9 Hz, =CH, central allylic proton), 6.52 (1 H, d, ³J(H–H) = 15.9 Hz, =CHPh, proton *trans* to the central allylic proton); MS data: *m/z* 201 (M⁺, 12%), 117 (44, M – NC₅H₁₀), 98 (16 M – CH=CHC₆H₅), 84 (9, M – CH₂CH=CHC₆H₅).

C₅H₁₀N–CMe₂–CH=CH₂ (3-methyl-3-piperidino-1-butene) δ_{H} (300 MHz, CDCl₃, 298 K): 1.18 (6 H, s, CH₃), 5.05 (1 H, d, ³J(H–H) = 17.4 Hz, =CH₂, proton *trans* to the central allylic proton), 5.08 (1 H, d, ³J(H–H) = 11.0 Hz, =CH₂ proton *cis* to the central allylic proton), 5.94 (1H, dd, =CH, central allylic proton), *cf.* the corresponding allyl proton resonances of the related compound Me₂N–CMe₂–CH=CH₂.³

X-ray crystallography

Intensity data for compound [Pd(η^1 -C₃H₅)(P–N–P′)]BF₄·0.25(Et₂O) were collected on an Oxford Diffraction Excalibur diffractometer using Mo K α radiation (λ = 0.71073 Å). The diffractometer was equipped with a cryocooling device which has been used to set the temperature at 150 K. Data collection was performed with the program CrysAlis CCD.¹⁷ Data reduction was carried out with the program CrysAlis RED.¹⁸ The absorption correction was applied using the ABSPACK program.¹⁹

The structure was solved by using the SIR-97 package²⁰ and subsequently refined on the *F*² values by the full-matrix least-squares program SHELXL-97.²¹

All the non-hydrogen atoms were refined anisotropically with the exception of those of the diethyl ether molecule, all the hydrogen atoms of the ligands were set in calculated positions and refined with an isotropic thermal parameter depending on the atom to which they are bound.

The diethyl ether non-hydrogen atoms were refined isotropically with an occupancy factor of 0.25, the hydrogen atoms of this molecule were not introduced in the refinement.

Geometrical calculations were performed by PARST97²² and molecular plots were produced by the ORTEP3 program.²³ Crystallographic data and refinement parameters are reported in Table 6.

Computational methods

The Gaussian 09 (revision B.01)²⁴ package was used. All the studied species were fully optimized by using the density functional theory (DFT) method by means of Becke's three-parameter hybrid method using the LYP correlation functional.²⁵ The effective core potential of Hay and Wadt²⁶ was used for the palladium atom. The 6-31G* basis set was used for the remaining atomic species.²⁷ The reliability of the found stationary points (minima on the potential energy surface) was assessed by evaluating the vibrational frequencies. Starting geometries for the

Table 6 Crystallographic data and refinement parameters for [Pd(η^1 -C₃H₅)(P–N–P′)]BF₄·0.25(Et₂O)

Chemical formula	[Pd(η^1 -C ₃ H ₅)(P–N–P′)](BF ₄)·0.25(Et ₂ O)
<i>M_r</i> /mol ^{−1}	802.36
Crystal size/mm	0.50 × 0.45 × 0.30
Crystal system	Triclinic
Space group	<i>P</i> 1
<i>a</i> /Å	11.0898(8)
<i>b</i> /Å	12.060(1)
<i>c</i> /Å	15.869(1)
α (°)	73.145(7)
β (°)	76.574(6)
γ (°)	81.511(7)
<i>U</i> /Å ³	1968.3(2)
<i>Z</i>	2
<i>D_c</i> /Mg m ^{−3}	1.6354
μ /mm ^{−1}	0.601
λ /Å	0.71073
<i>T</i> /K	150
2 θ range (°)	8.4–57.8
Index range (<i>hkl</i>)	−14 to 13 −16 to 15 −21 to 19
Reflections collected/unique	15 832/8511
Goodness-of-fit on <i>F</i> ²	0.932
<i>R</i> ₁ , <i>wR</i> ₂ [<i>I</i> > 2 σ (<i>I</i>)]	0.0861/0.1660
<i>R</i> ₁ , <i>wR</i> ₂ [all data]	0.1795/0.1943
$\Delta\rho_{\text{max/min}}$ /e Å ^{−3}	0.921/−0.770

modelled species (**1I**, **3I**, **3II** and **4I**, **4II**) were based on X-ray diffraction data about analogous species, where available.

Acknowledgements

CRIST (Centro di Cristallografia Strutturale), University of Florence, where the X-ray measurements were performed is gratefully acknowledged.

References

- (a) J. Powell and B. L. Shaw, *J. Chem. Soc. A*, 1967, 1839–1851; (b) S. Numata, R. Okawara and H. Kurosawa, *Inorg. Chem.*, 1977, **16**, 1737–1741; (c) H. Kurosawa, A. Urabe, K. Miki and N. Kasai, *Organometallics*, 1986, **5**, 2002–2008; (d) P. K. Byers and A. J. Canty, *J. Chem. Soc., Chem. Commun.*, 1988, 639–641; (e) R. E. Rülke, D. Kliphuis, C. J. Elsevier, J. Fraanje, K. Goubitz, P. W. N. M. van Leeuwen and K. Vrieze, *J. Chem. Soc., Chem. Commun.*, 1994, 1817–1819; (f) P. Wehman, R. E. Rülke, V. E. Kaasjager, P. C. J. Kamer, H. Kooijman, A. L. Spek, C. J. Elsevier, K. Vrieze and P. W. N. M. van Leeuwen, *J. Chem. Soc., Chem. Commun.*, 1995, 331–332; (g) R. E. Rülke, V. E. Kaasjager, P. Wehman, C. J. Elsevier, P. W. N. M. van Leeuwen, K. Vrieze, J. Fraanje, K. Goubitz and A. L. Spek, *Organometallics*, 1996, **15**, 3022–3031; (h) J. Krause, R. Goddard, R. Mynott and K.-R. Pörschke, *Organometallics*, 2001, **20**, 1992–1999; (i) T. Cantat, E. Génin, C. Giroud, G. Meyer and A. Jutand, *J. Organomet. Chem.*, 2003, **687**, 365–376; (j) N. Solin, J. Kjellgren and K. J. Szabó, *J. Am. Chem. Soc.*, 2004, **126**, 7026–7033.
- (a) S. Ramdeehul, L. Barloy, J. A. Osborn, A. De Cian and J. Fischer, *Organometallics*, 1996, **15**, 5442–5444; (b) L. Barloy, S. Ramdeehul, J. A. Osborn, C. Carlotti, F. Taulelle, A. De Cian and J. Fischer, *Eur. J. Inorg. Chem.*, 2000, 2523–2532; (c) P. Braunstein, F. Naud, A. Dedieu, M.-M. Rohmer, A. De Cian and S. J. Retting, *Organometallics*, 2001, **20**, 2966–2981; (d) M. Kollmar and G. Helmchen, *Organometallics*, 2002, **21**, 4771–4775; (e) P. Braunstein, J. Zhang and R. Welter, *Dalton Trans.*, 2003, 507–509; (f) B. Goldfuss, T. Löschmann and F. Rominger, *Chem.–Eur. J.*, 2004, **10**, 5422–5431; (g) J. Zhang, P. Braunstein and R. Welter, *Inorg. Chem.*, 2004, **43**, 4172–4177; (h) J. I. van der Vlugt, M. A. Siegler, M. Jansen, D. Vogt and A. Spek,

- Organometallics*, 2009, **28**, 7025–7032; (i) B. Crociani, S. Antonaroli, M. Burattini, P. Paoli and P. Rossi, *Dalton Trans.*, 2010, **39**, 3665–3672; (j) L. Canovese, F. Visentin, C. Santo, G. Chessa and V. Bertolasi, *Organometallics*, 2010, **29**, 3027–3038.
- 3 B. Åkermark, G. B. Åkermark, L. S. Egedus and K. Zetterberg, *J. Am. Chem. Soc.*, 1981, **103**, 3037–3040.
- 4 (a) M. García-Iglesias, E. Buñuel and D. J. Cárdenas, *Organometallics*, 2006, **25**, 3611–3618; (b) P. Fristrup, M. Ahlquist, D. Tanner and P.-O. Norrby, *J. Phys. Chem.*, 2008, **112**, 12862–12867.
- 5 (a) K. Szabó, *Chem.–Eur. J.*, 2000, **6**, 4413–4421; (b) O. A. Wallner and K. Szabó, *Org. Lett.*, 2002, **4**, 1563–1566; (c) O. A. Wallner and K. Szabó, *Chem.–Eur. J.*, 2003, **9**, 4025–4230; (d) O. A. Wallner and K. Szabó, *J. Org. Chem.*, 2002, **68**, 2934–2943; (e) N. Solin, O. A. Wallner and K. Szabó, *Org. Lett.*, 2005, **7**, 689–691.
- 6 (a) B. Crociani, S. Antonaroli, L. Canovese, P. Uguagliati and F. Visentin, *Eur. J. Inorg. Chem.*, 2004, 732–742; (b) A. Scrivanti, V. Beghetto, U. Matteoli, S. Antonaroli, A. Marini and B. Crociani, *Tetrahedron*, 2005, **61**, 9752–9758; (c) B. Crociani, S. Antonaroli, A. Marini, U. Matteoli and A. Scrivanti, *Dalton Trans.*, 2006, 2698–2705; (d) A. Scrivanti, M. Bertoldini, U. Matteoli, S. Antonaroli and B. Crociani, *Tetrahedron*, 2009, **65**, 7611–7615.
- 7 E. W. Ainscough, A. M. Brodie, A. K. Burrell, A. Derwall, G. B. Jameson and S. K. Taylor, *Polyhedron*, 2004, **23**, 1159–1168.
- 8 M. Hesse, H. Meier and B. Zech, *Metodi Spettroscopici nella Chimica Organica*, EdiSES, Napoli, 5th edn, 1996, ch. 3, p. 99.
- 9 (a) U. C. Singh and P. A. Kollman, *J. Comput. Chem.*, 1984, **5**, 129–145; (b) B. H. Besler, K. M. Merz Jr. and P. A. Kollman, *J. Comput. Chem.*, 1990, **11**, 431–439.
- 10 (a) S. Doherty, J. G. Knight, T. H. Scanlan, M. R. J. Elsegood and W. J. Clegg, *J. Organomet. Chem.*, 2002, **650**, 231–248; (b) E. W. Ainscough, A. M. Brodie, A. K. Burrell, A. Derwahl and S. K. Taylor, *Inorg. Chim. Acta*, 2004, **357**, 2379–2384.
- 11 Structures found in the Cambridge Structural Database (CSD, v. 5.32): F. H. Allen, *Acta Crystallogr., Sect. E: Struct. Rep. Online*, 2002, **B58**, 380–388.
- 12 D. Cremer and J. A. Pople, *J. Am. Chem. Soc.*, 1975, **97**, 1354–1358.
- 13 C. Janiak, *J. Chem. Soc., Dalton Trans.*, 2000, 3885–3896.
- 14 B. Crociani, S. Antonaroli, L. Canovese, F. Visentin and P. Uguagliati, *Inorg. Chim. Acta*, 2001, **315**, 172–182.
- 15 (a) R. Hartley and S. R. Jones, *J. Organomet. Chem.*, 1974, **66**, 465–473; (b) M. C. Ashraf, T. G. Burrowes and W. R. Jackson, *Aust. J. Chem.*, 1976, **29**, 2643–2649.
- 16 E. W. Ainscough, A. M. Brodie, P. D. Buckley, A. K. Burrell, S. T. F. Kennedy and J. M. Waters, *J. Chem. Soc., Dalton Trans.*, 2000, 2663–2671.
- 17 *CrysAlis CCD, Version 1.171.pre23_10 beta*, Oxford Diffraction Ltd (release 21.06.2004 CrysAlis171.NET) (compiled June 21, 2004, 12:00:08).
- 18 *CrysAlis RED, Version 1.171.pre23_10 beta*, Oxford Diffraction Ltd (release 21.06.2004 CrysAlis171.NET) (compiled June 21, 2004, 12:00:08).
- 19 *ABSPACK in CrysAlis RED, Version 1.171.29.2*, Oxford Diffraction Ltd (release 20.01.2006 CrysAlis171.NET), (compiled January 20, 2006, 12:36:28).
- 20 M. C. Burla, M. Camalli, B. Carrozzini, G. L. Casciarano, C. Giacovazzo, G. Polidori and R. Spagna, *J. Appl. Crystallogr.*, 2003, **36**, 1103.
- 21 G. M. Sheldrick, *Acta Crystallogr., Sect. A: Fundam. Crystallogr.*, 2008, **A64**, 112–122.
- 22 M. Nardelli, *J. Appl. Crystallogr.*, 1995, **28**, 659.
- 23 L. J. Farrugia, *J. Appl. Crystallogr.*, 1997, **30**, 565.
- 24 M. J. Frisch, G. W. Trucks, H. B. Schlegel, G. E. Scuseria, M. A. Robb, J. R. Cheeseman, G. Scalmani, V. Barone, B. Mennucci, G. A. Petersson, H. Nakatsuji, M. Caricato, X. Li, H. P. Hratchian, A. F. Izmaylov, J. Bloino, G. Zheng, J. L. Sonnenberg, M. Hada, M. Ehara, K. Toyota, R. Fukuda, J. Hasegawa, M. Ishida, T. Nakajima, Y. Honda, O. Kitao, H. Nakai, T. Vreven, J. A. Montgomery, Jr., J. E. Peralta, F. Ogliaro, M. Bearpark, J. J. Heyd, E. Brothers, K. N. Kudin, V. N. Staroverov, T. Keith, R. Kobayashi, J. Normand, K. Raghavachari, A. Rendell, J. C. Burant, S. S. Iyengar, J. Tomasi, M. Cossi, N. Rega, J. M. Millam, M. Klene, J. E. Knox, J. B. Cross, V. Bakken, C. Adamo, J. Jaramillo, R. Gomperts, R. E. Stratmann, O. Yazyev, A. J. Austin, R. Cammi, C. Pomelli, J. W. Ochterski, R. L. Martin, K. Morokuma, V. G. Zakrzewski, G. A. Voth, P. Salvador, J. J. Dannenberg, S. Dapprich, A. D. Daniels, O. Farkas, J. B. Foresman, J. V. Ortiz, J. Cioslowski and D. J. Fox, Gaussian, Inc., Wallingford CT, 2010.
- 25 A. D. Becke, *J. Chem. Phys.*, 1993, **98**, 5648–5652.
- 26 P. J. Hay and W. R. Wadt, *J. Chem. Phys.*, 1985, **82**, 299–310.
- 27 G. A. Petersson, A. Bennett, T. G. Tensfeldt, M. A. Al-Laham, W. A. Shirley and J. Mantzaris, *J. Chem. Phys.*, 1988, **89**, 2193–2218.